

UC Berkeley

UC Berkeley Previously Published Works

Title

Personal Exposure to PM2.5 Black Carbon and Aerosol Oxidative Potential using an Automated Microenvironmental Aerosol Sampler (AMAS).

Permalink

<https://escholarship.org/uc/item/1c14g18b>

Journal

Environmental Science & Technology, 52(19)

Authors

Quinn, Casey
Miller-Lionberg, Daniel
Klunder, Kevin
et al.

Publication Date

2018-10-02

DOI

10.1021/acs.est.8b02992

Peer reviewed



HHS Public Access

Author manuscript

Environ Sci Technol. Author manuscript; available in PMC 2019 October 02.

Published in final edited form as:

Environ Sci Technol. 2018 October 02; 52(19): 11267–11275. doi:10.1021/acs.est.8b02992.

Personal Exposure to PM_{2.5} Black Carbon and Aerosol Oxidative Potential using an Automated Microenvironmental Aerosol Sampler (AMAS)

Casey Quinn[†], Daniel D. Miller-Lionberg[‡], Kevin J. Klunder[§], Jaymin Kwon^{||}, Elizabeth M. Noth[⊥], John Mehaffy[‡], David Leith^{‡, #}, Sheryl Magzamen[†], S. Katharine Hammond[⊥], Charles S. Henry^{*, §}, and John Volckens^{*, †, ‡}

[†] Department of Environmental and Radiological Health Sciences, Colorado State University, Fort Collins, Colorado 80523, United States

[‡] Department of Mechanical Engineering, Colorado State University, Fort Collins, Colorado 80523, United States

[§] Department of Chemistry, Colorado State University, Fort Collins, Colorado 80523, United States

^{||} Department of Public Health, California State University, Fresno, California 93740, United States

[⊥] Environmental Health Sciences Division, School of Public Health, University of California, Berkeley, California 94720, United States

[#] Department of Environmental Sciences and Engineering, University of North Carolina at Chapel Hill, Chapel Hill, North Carolina 27599, United States

Abstract

Traditional methods for measuring personal exposure to fine particulate matter (PM_{2.5}) are cumbersome and lack spatiotemporal resolution; methods that are timeresolved are limited to a single species/component of PM. To address these limitations, we developed an automated microenvironmental aerosol sampler (AMAS), capable of resolving personal exposure by microenvironment. The AMAS is a wearable device that uses a GPS sensor algorithm in conjunction with a custom valve manifold to sample PM_{2.5} onto distinct filter channels to evaluate home, school, and other (e.g., outdoors, in transit, etc.) exposures. Pilot testing was conducted in Fresno, CA where 25 high-school participants ($n = 37$ sampling events) wore an AMAS for 48-h periods in November 2016. Data from 20 (54%) of the 48-h samples collected by participants were deemed valid and the filters were analyzed for PM_{2.5} black carbon (BC) using light transmissometry and aerosol oxidative potential (OP) using the dithiothreitol (DTT) assay. The

^{*} **Corresponding Authors** Phone: 1-970-491-6341; john.volckens@colostate.edu (J.V.). Phone: 1-970-491-2852; chuck.henry@colostate.edu (C.S.H.).

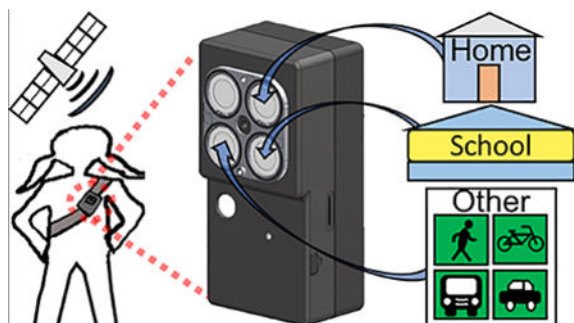
The authors declare no competing financial interest.

Supporting Information

The Supporting Information is available free of charge on the ACS Publications website at DOI: 10.1021/acs.est.8b02992. 18 figures, 9 equations, 1 table, and 1 method (PDF) AE33 ambient black carbon data for November 2016, the ambient PM_{2.5} data for November 2016, the AMAS data, and the reference sampler data on individual sheets (XLSX) surveys for the AMAS and the traditional personal reference sampler (PDF)

amount of inhaled $PM_{2.5}$ was calculated for each microenvironment to evaluate the health risks associated with exposure. On average, the estimated amount of inhaled $PM_{2.5}$ BC ($\mu g \text{ day}^{-1}$) and OP [$(\mu M \text{ min}^{-1}) \text{ day}^{-1}$] was greatest at home, owing to the proportion of time spent within that microenvironment. Validation of the AMAS demonstrated good relative precision (8.7% among collocated instruments) and a mean absolute error of 22% for BC and 33% for OP when compared to a traditional personal sampling instrument. This work demonstrates the feasibility of new technology designed to quantify personal exposure to $PM_{2.5}$ species within distinct microenvironments.

Graphic Abstract



INTRODUCTION

Particulate matter (PM) air pollution is the leading environmental risk factor for global morbidity and mortality.¹ Evidence connecting PM exposure and adverse health effects has been gathered primarily from studies that rely upon fixed, outdoor PM monitoring sites to estimate air pollution exposure.^{2–5} Although central-site monitoring is an effective way to estimate population-level exposures, such monitors are largely ineffective at estimating personal exposure, as PM tends to be spatially and temporally heterogeneous and because individuals are frequently moving from one microenvironment (e.g., home, school, other) to the next.^{6–10} Thus, studies that use central-site monitors to estimate air pollution effects at the individual level often suffer from exposure misclassification.¹¹

More recently, exposure modeling frameworks, such as temporal land-use regression, have been developed to estimate individual exposure on finer spatial and temporal scales.^{12–16}

These advanced spatiotemporal models, however, also struggle to capture the known variability in individual-level PM exposure.^{17–19} Alternatively, personal exposure monitoring (i.e., using a wearable device to measure PM within an individual's breathing zone), represents a direct measure of an individual's exposure to PM.^{20,21} The use of active-sampling personal monitors also permits the evaluation of PM composition (i.e., black carbon [BC], organic compounds, metals, and aerosol oxidative potential [OP]).^{22–24}

Personal sampling technologies, however, have a number of limitations. Traditional personal samplers, for example, collect one time-integrated sample per measurement (i.e., PM is collected onto a single filter substrate); thus, exposure cannot be resolved spatially or

temporally.²⁵ To address this limitation, studies have either paired multiple filter samplers together to resolve exposures by microenvironment²⁶ or coupled a direct-reading instrument with a global positioning system (GPS) to resolve these exposures with data processing/analyses.^{27–29} Though direct-reading instruments can provide time-resolved exposure data, these instruments tend to be expensive (limiting sample size) and often report only levels of a single species (e.g., PM_{2.5} mass or black carbon [BC]).^{30–34} Finally, many personal samplers are bulky, noisy, and intrusive leading to low rates of compliance among participants.³⁴ These limitations highlight a need for personal PM monitors that are inexpensive, wearable, and capable of resolving speciated PM exposures as a function of distinct microenvironments—the goal of this work.

The Automated Microenvironmental Aerosol Sampler (AMAS) is a wearable, active aerosol sampling device containing four separate filter channels. Each filter channel is used to sample fine particulate matter (PM_{2.5}) from predetermined personal microenvironments based on global positioning system (GPS) location. We evaluated the ability of the AMAS to determine personal exposures by microenvironment (home, school, and other) in a pilot study with high school students in Fresno, California. Collected PM_{2.5} filter samples ($n = 126$ microenvironments) were evaluated for both BC^{35–37} and OP^{38–40} using established methods.

MATERIALS AND METHODS

Hardware.

The AMAS (Figure 1, Figure S1 and Table S1 of the Supporting Information, SI) was designed to be small enough ($105 \times 51 \times 56 \text{ mm}^3$) and light enough (240 g) to be worn by school-aged children (i.e., ages ~7–18 yrs). The AMAS pump and flow-control systems are derived from previous efforts to develop a single-filter PM_{2.5} sampler called the Ultrasonic Personal Aerosol Sampler (UPAS).⁴¹ The UPAS is a wearable, filter-based aerosol sampler that contains a piezoelectric micropump, a mass flow sensor, and a suite of environmental sensors (temperature, pressure, relative humidity, acceleration, and light). A key feature of the UPAS pump is that it operates at ultrasonic frequency, producing low noise (<55 dB) in a compact form factor.⁴¹ The AMAS is differentiated from the UPAS by the addition of a global navigation satellite system (GNSS CAM-M8Q, Ublox, Thalwil, Switzerland) and a novel, four-channel flow manifold: each channel is comprised of a separate PM_{2.5} cyclone inlet (1.5 L min^{-1} flow rate, Figure S2) and a 15 mm sampling filter. Airflow through each channel is controlled by a customdesigned valve manifold (Figure 1B). This manifold contains four miniature planetary gear motors (206–108, Precision Microdrives, London, U.K.), each connected to a custommachined axial valve that lies between the pump manifold and a given inlet. The four valves are actuated independently by a microcontroller algorithm (described below) to allow airflow through a single filter channel on demand.

The inlet manifold consists of a single aluminum filter holder that houses all four filters, integrates the cyclone inlets into a single combined inlet and cover to make the device more aesthetically pleasing, and also contains multidirectional air inlet paths to reduce the possibility of blocked air flow during use. The AMAS is powered by two batteries

(SAEBBG900BBU, Samsung, Seoul, South Korea) that can be recharged (even while sampling) via a standard micro-USB connection.

Firmware.

The AMAS functionality is controlled with firmware developed for a microcontroller (mbed; ARM, Ltd., Cambridge, U.K.) that has been integrated into a printed circuit board (Figure 1A). The firmware enables AMAS setup and programming via Bluetooth and in conjunction with a smartphone application (Android⁴² and iOS⁴³ versions; see Figure S3 for screenshots of the app interface). The app allows the user to input microenvironment GPS coordinates, set basic operational settings, and initiate sampling (each of these settings are stored in nonvolatile memory). Participants did not carry a smartphone with the app installed, all AMAS programming and smartphone app use was limited to the research staff, and no data were collected or transferred using the smartphone app. Additionally, the AMAS firmware implements the microenvironmental algorithm, regulates sample volumetric flow rate, and monitors battery life. A multicolor light-emitting diode on the exterior of the upper housing serves as a visual indicator (to the user) about the operational state of the AMAS. A green light indicates normal operation, a blue light is shown while the AMAS is charging, a yellow light is displayed when the battery is under ~20% charge, and the light turns red when the pumps shut down (~10% of battery charge). Shutting the pumps off when the batteries are critically low impacts the sample time, but allows all AMAS sensors (other than the pumping system) to remain operational and continue to log data until the device can be charged. Sensors data are logged to nonvolatile memory at 0.2 Hz, with the exception of the total acceleration (square root of the sum of the squares of the three acceleration axes) and light sensor data (ultraviolet, visible, and infrared), which were logged at 1 Hz.

Algorithm.

A key element of the AMAS is the ability to collect multiple PM_{2.5} samples by time or location with the same personal sampler. The AMAS real-time clock could be leveraged and the firmware can be modified to have the filter channels collect at specific times of day. This could be permanently programmed into the device firmware or programmed such that these times could be modified using the smartphone application. However, for this study, we developed an algorithm that can detect predefined microenvironments based on location and environmental sensor data. The work described here sampled PM_{2.5} from three microenvironments: (1) “home”—a 75 m radius around the central point of the home; (2) “school”—a 100 m radius around the central point of the school; and (3) “other”— anytime the AMAS was not located in either the home or school microenvironments. Prior to sampling, the GPS coordinates corresponding to the participant’s home and school were determined using Google Maps and programmed into the AMAS via the smartphone application by a member of the research team. The algorithm could accept two home and two school locations for each participant. In cases where a child spent time in two home locations, these were considered as a single microenvironment (i.e., the samples from both homes were collected on the same filter). The same procedure was applied to the school microenvironment because participating students traveled between two different schools (their primary school and the Center for Advanced Research and Technology [CART],

where the participants visited each day and also where they received and returned the AMAS) during the 48-h sampling period.

The microenvironment detection algorithm used logic tied to the on-board GPS to estimate when an individual entered or exited a given microenvironment; the flowchart, shown in Figure 2, outlines this algorithm. The first decision point in the algorithm was to determine the presence of a GPS signal. If a signal was detected and had been present for at least 50 s, then the radial distances to the home and school central points were calculated. If the calculated distance was less than 75 m from a home location or less than 100 m from a school location, then the appropriate filter channel (home or school) was activated. If neither a home nor a school microenvironment was detected, then the filter channel designated as other was activated. In the cases where no GPS signal was acquired, then the last known location was used. If the last known location was >100 m from a school or >75 m from a home microenvironment, then the “other” filter channel was used.

Sample Collection.

High school students between the ages of 16 and 18 were recruited from CART in Fresno, CA to evaluate the AMAS. Each student wore the AMAS for a 48-h monitoring period and students were eligible to participate in the pilot multiple times. All study procedures were approved by the Institutional Review Board at the University of California at Berkeley and participants either provided informed consent or assent with consent from their parent/guardian.

For each 48-h sample period, five reference samplers were deployed alongside five AMAS prototypes (assigned to participants at random) to compare performance. The reference sampler consisted of a backpack containing a traditional personal sampler with a PM_{2.5} size-selective inlet (PEM 761–203A, SKC, Inc., Eighty Four, PA, U.S.A.), a personal sampling pump (BGI OMNI 3000, Mesa Laboratories, Lakewood, CO, U.S.A.), and a 25 mm filter cassette (Figure S4). The AMAS filters were cut from Pallflex Fiberfilm (T60A20; Pall Life Sciences, Ann Arbor, MI) sheets using a 15 mm punch. The reference sampler used 25 mm filters cut from Pallflex Fiberfilm sheets (10 of 15) and 25 mm Teflon filters (5 of 15; PT25P-PF03; Measurement Technology Laboratories (MTL), Minneapolis, MN). The reference filter samples were collected at 4 L min⁻¹, while the AMAS collected filter samples at 1.5 L min⁻¹. Additionally, a research team member collocated and transported five AMAS between microenvironments for 48 h to evaluate instrument precision. After sampling, filters were sealed in plastic cassettes and stored at -20 °C until they were shipped to Colorado State University and analyzed for BC and OP (within 3 months of sample collection). At the conclusion of each sampling event, all of the data logged to the AMAS were removed from the AMAS solidstate memory and transferred to a secure server.

AMAS Evaluation.

The AMAS battery life, power failure rate, and microenvironment detection algorithm were evaluated as part of the pilot study. Logged readings of AMAS pump and battery status were used to determine the AMAS battery life and power failure rate. The raw data from the GNSS module integrated in the AMAS were used to evaluate the microenvironment

designations determined with the algorithm for bad transitions (instances where the algorithm detected a home-to-school or school-to-home transition without detecting a transition to the other microenvironment). Additionally, the distances from the home and school microenvironments at the time of a transition from either a home or school to the other microenvironment were analyzed to evaluate the responsiveness of the algorithm.

Black Carbon Analysis.

Black carbon loading on each sampling filter was assessed by optical transmissometry at 880 nm (SootScan OT-21, Magee Scientific, Berkeley, CA, U.S.A.). Mass absorption cross sections of 12.2^{45} and 9.18^{37} $\text{cm}^2 \mu\text{g}^{-1}$ were used for the Pallflex Fiberfilm and MTL Teflon filters, respectively, following published data for the differential absorption properties of these filters. The 25 mm filters used a standard filter holder provided by Magee Scientific; however, the 15 mm filters required a custom aluminum filter holder. The custom filter holder (Figure S5) was designed with computer-aided design software (SolidWorks ANSYS, Inc., Canonsburg, PA, U.S.A.) and machined specifically for this study. Each filter was scanned twice; once prior to sampling and once after the 48-h collection period. The Teflon filters were analyzed with a Pallflex Fiberfilmfilter underneath (as a light diffuser) per the protocol described by Presler-Jur et al.³⁷ The BC filter mass, concentrations, and daily inhaled mass were calculated using eqs S1, S2, and S3. An inhalation rate of $16.3 \text{ m}^3 \text{ day}^{-1}$ determined by the U.S. Environmental Protection Agency for 16 to 21 year olds⁴⁶ was used in eq S3 to determine the daily inhaled BC mass for each participant by microenvironment. Laboratory filter blanks (15 mm and 25 mm) were stored in filter keepers and measured at least once each day that filters were analyzed. These laboratory blanks were used to determine the limit of detection ($3 \times$ blank standard deviation) for the optical method. For the 15 AMAS/ reference sampler pairs, the cumulative AMAS BC concentration ($\mu\text{g m}^{-3}$) of the three 15 mm filters (eq S4) was compared to the corresponding 25 mm reference sampler filter concentration estimate.

Ambient BC measurements were recorded using the 880 nm channel of a Magee Scientific Aethalometer (AE33, Berkeley, CA, U.S.A.), which was installed, maintained, and monitored by the UC Berkeley-Stanford Children's Environmental Health Center at the California Air Resources Board (CARB) FresnoGarland monitoring station (Air Quality System [AQS] site 060190011). Hourly BC concentrations reported by the AE33 instrument were used to estimate the mass of BC that would be captured on the AMAS filter if the AMAS had been located at the central site location operating at flow of 1.5 L min^{-1} . Ambient $\text{PM}_{2.5}$ concentrations (hourly averages) were also obtained from the AQS Web site for the month of November 2016. Data were aggregated to 24-h averages and compared to the AE33 BC data to determine the mean ambient BC: $\text{PM}_{2.5}$ ratio during the study.

Oxidative Potential Analysis.

The oxidative potential (OP) of PM, which can contain or can lead to the formation of reactive oxygen species in the body, is a marker of PM toxicity.^{47,48} The oxidative potential of $\text{PM}_{2.5}$ collected on sampling filters was estimated using the dithiothreitol (DTT) assay. The 15 mm filters were first cut in half and the 25 mm filters were quartered with ceramic scissors; the filter half or quarter were used for the DTT analysis. A DTT analysis method

(SI for details) similar to the traditional method⁴⁹ was used to determine the OP. The four absorbance measurements for each filter sample were used to calculate the consumption rate of DTT. Additionally, laboratory filter blanks were analyzed with this method, and the OP results were adjusted by the mean DTT consumption rate of the laboratory blanks to account for the reactivity contribution of the filter substrate. The OP for the mass collected on the filters, adjusted for air sample volume (concentration), and daily inhaled PM_{2.5} were calculated for each microenvironment using eqs S5, S6, S7, and S8. For the 15 AMAS/reference sampler pairs, the cumulative AMAS OP concentration (pmol min⁻¹ m⁻³) of the three 15 mm filters (Equation S9) was compared to the corresponding 25 mm reference sampler estimates.

Data Analysis.

The Kruskal–Wallis test and pairwise Wilcoxon sign rank were used to test for significant differences between microenvironments for the BC and OP analyses. Deming regressions, concordance coefficient correlations (CCC), Bland-Altman limits of agreements (LoA), normalized mean bias factors (B_{NMBF}),⁵⁰ normalized mean absolute error factors (E_{NMAEF}),⁵⁰ and mean normalized absolute errors (MNAE) were used to evaluate AMAS accuracy as compared to a traditional personal sampler, with a goal of achieving ±25% accuracy per established guidelines for personal exposure monitoring.⁵¹ The relative standard deviation of the black carbon analysis for the five collocated AMAS was used to evaluate precision. All data processing and analyses were conducted using R 3.4.1 (R Core Team, Vienna, Austria).

RESULTS AND DISCUSSION

AMAS Performance.

The AMAS devices were deployed with participants a total of 37 times over the course of the pilot study (15 deployments were paired with a traditional personal sampler for reference). An additional five AMAS were collocated on a single backpack by a member of the research team, resulting in 42 AMAS deployments in total ($n = 126$ microenvironmental filters; 15 reference filters). On average, the AMAS battery lasted 14 h at 1.5 L min⁻¹; however, asking participants to charge the device overnight resulted in most deployments meeting the target sampling time (48 h). A total of 88% of AMAS (37 of the 42) logged data for at least 90% of the time (>43.2 h) and all 37 of those logged for the entire 48h period; however, only 71% (30 of the 42) of the AMAS logged and sampled for greater than 90% of the 48-h period (43.2 h). Of these, 64% (27 of the 42) sampled and logged for the entire 48-h period. Two additional deployments had incorrect microenvironment GPS coordinates programmed into the AMAS (the incorrect GPS coordinates were due to user error). Thus, the data from 20 deployments (54%) with student participants and the test with five AMAS collocated by a researcher were deemed valid for analysis.

Our analyses of BC and OP exposure levels were restricted to AMAS filter samples (59 of 126 filters from 20 of 42 deployments) that met the following quality criteria: collected by student participants, logged data for the entire 48-h period, had valid microenvironment GPS coordinates, and collected PM_{2.5} for more than an hour (i.e., a sample volume >0.1 m³) in each microenvironment. For these 59 valid AMAS filters, the median (25th, 75th) amount

of time spent in the school, home, and other microenvironments as determined by the algorithm were 4.9 (3.9, 5.6) hrs day⁻¹, 15.5 (13.5, 16.4) hrs day⁻¹, and 4.4 (3.4, 5.8) hrs day⁻¹, respectively (Figure 3A).

The time sampled in each microenvironment was checked against the raw GPS data to evaluate the performance of the AMAS algorithm. The use of a predetermined radius about the centroids of the home and school microenvironments (75 and 100 m, respectively) successfully detected the majority of the time when participants were present in these two locations. However, this approach was imprecise when the GPS signal drift was high, when the home microenvironment consisted of larger multifamily dwellings, and because of the large footprint and open-building design (lack of internal hallways) of California high schools. A hypothesis is that the latter reason is why the estimated time spent at school seems lower than anticipated (7–8 h per day) and the estimated time spent in the “other” microenvironment was higher than anticipated. Additionally, the time to acquire a GPS signal (distance from the home and school microenvironments) was another infrequent (33 of 780 transitions for 22 of 42 deployments), but key issue that was observed. An empirical cumulative distribution of the distance (in meters) from the prior microenvironment when the AMAS transitioned to a new microenvironment is shown in Figure S6. This analysis reveals a key issue when relying on GPS data as the primary determinant of microenvironment transition: limited or no satellite connection results in error due to a delayed transition. The limitations of relying solely on the GPS to detect microenvironments was anticipated as this challenge has been discussed in previous studies that have used GPS for microenvironment classification.^{19,27,28,52} The reliance of only GPS location for microenvironment classification was merely a starting point for the AMAS development, and improvement of the microenvironment detection algorithm is the subject of ongoing work. For example, further refinement of the GPS settings and the use of other environmental sensors (e.g., ultraviolet light intensity, acceleration, temperature, etc.) may help improve the ability to detect a change in microenvironment when GPS signals are weak.

Black Carbon (BC).

Most home filter samples (18 of 19) exceeded the method limit of detection (LOD) for BC (0.49 μg) as compared to fewer school (9 of 20) and other (12 of 20) filter samples. BC exposure concentrations are provided in Figure S7. Median (25th, 75th%) levels of BC concentrations were 0.4 (0.3, 0.6) $\mu\text{g m}^{-3}$ for school, 1.4 (0.8, 2.2) $\mu\text{g m}^{-3}$ for home, and 0.6 (0.3, 0.8) $\mu\text{g m}^{-3}$ for “other”. Inhaled BC mass is shown in Figure 3B for each of the three microenvironments. Median (25th, 75th%) levels of inhaled BC mass were 1.6 (1.1, 2.4) $\mu\text{g day}^{-1}$ for school, 5.4 (2.9, 8.2) $\mu\text{g day}^{-1}$ for home, and 2.2 (1.3, 3.1) $\mu\text{g day}^{-1}$ for “other”. Inhaled BC mass was significantly higher in home versus both school and “other” microenvironments (pairwise Wilcoxon sign rank; $p < 0.001$), even though BC exposure concentrations tended to be similar across microenvironments (Kruskal–Wallis Test; $p = 0.5$), as shown in Figure S7. This discrepancy is explained by the fact that participants spent the majority of their time (~65%) at home. One option for improving BC detection would be to increase the amount of sample mass on the school and other filters by increasing the flow

through those filter channels and use a modified PM_{2.5} cyclone inlet suitable for the modified flow rate.

Oxidative Potential (OP).

Similar to BC, the OP home filters (17 of 19) had the greatest number of filter samples with a measured response, within error, above the blank ($0.34 \mu\text{M min}^{-1}$) compared to the school (11 of 20) and “other” filters (15 of 20). When normalized to sampled air volume (Figure S8), the median OP (25th, 75th%) concentrations were 165 (129, 269) [$\text{pmol min}^{-1} \text{m}^3$] for school, 135 (113, 189) [$\text{pmol min}^{-1} \text{m}^3$] for home, and 266 (132, 374) [$\text{pmol min}^{-1} \text{m}^3$] for other. These values are similar to those previously reported for urban, rural, or roadside PM (50–1500 $\text{pmol min}^{-1} \text{m}^{-3}$).⁴⁰ OP for inhaled PM_{2.5} is shown by microenvironment in Figure 3C, and the median inhaled OP (25th, 75th%) values were 1.2 (0.8, 1.8) [$(\mu\text{M min}^{-1}) \text{day}^{-1}$] for school, 2.5 (2.2, 3.1) [$(\mu\text{M min}^{-1}) \text{day}^{-1}$] for home, and 1.4 (1.1, 2.4) [$(\mu\text{M min}^{-1}) \text{day}^{-1}$] for other. The OP for inhaled PM_{2.5} in the home microenvironment was significantly greater than the exposure in the school microenvironment (pairwise Wilcoxon sign rank; $p < 0.001$), while there was no significant difference for OP concentrations (Kruskal–Wallis Test; $p = 0.07$). The variability in the OP measurement was relatively high, especially for filters that sampled lower air volumes, as shown in Figure S9. Future work should aim to increase the minimum sampled air volume and/or increase assay sensitivity to reduce error in the DTT assay. If future sample collection aimed to collect a minimum sampled mass equal to the BC LOD ($0.49 \mu\text{g}$), this would equate to $11.2 \mu\text{g PM mL}^{-1}$ in the DTT assay (based on an estimated ambient BC:PM ratio of 0.04 and a $500 \mu\text{L}$ dilution volume for the DTT assay), near $10 \mu\text{g mL}^{-1}$ as previously recommended for the DTT assay.³⁹

Instrumentation Exposure Comparisons.

The BC results for the 15 deployments that had an AMAS paired with a backpack containing a traditional personal sampler is shown in Figure 4. The gray bars represent the 48-h average BC concentration of the 25 mm reference sampler filters. The multicolored bars represent the BC concentration fraction on each of the three AMAS filters (shown as a summation of the three microenvironments BC mass in μg divided by the total sampled volume for the 48-h period). The percent error between the reference sampler and cumulative AMAS BC concentrations are shown above each paired filter set. The 12 data pairs with complete 48-h deployments (excluding three pairs [2, 11, 15] which had reference sampler pump failures) were used to evaluate the accuracy of the AMAS as compared to the traditional personal sampler used as a reference. The error (MNAE = 22% and $E_{\text{NMAEF}} = 0.099$) for these data pairs and a Deming regression (Figure S10) demonstrate a minor overestimation by the AMAS, moderate correlation ($r = 0.67$, CCC = 0.63) and a low bias demonstrated by the BlandAltman plot (Figure S11, LoA = $[-0.30, 0.20 \mu\text{g m}^{-3}]$, $B_{\text{NMBF}} = 0.099$). In addition, the five filter samples collected for the home microenvironment by the five collocated AMAS were above the BC LOD and demonstrated a good agreement (Figure S12 and S13) for microenvironment BC mass and concentration estimates (relative standard deviation of 8.7% and 8.8%, respectively) between AMAS, thus demonstrating AMAS precision. These results suggest that the AMAS can provide similar BC results as a traditional personal sampler. Following the BC analysis, the OP for the 15 AMAS/reference

sampler pairs were compared (Figures 4 and S14). The gray bars represent the 48-h OP of the 25 mm reference sampler filters. The multicolored bars represent the OP fraction on the AMAS filters (shown as a summation of the three microenvironments OP in $\mu\text{M min}^{-1}$ divided by the total sampled volume for the 48-h period). In addition to the three reference sampler deployments that had pump failures, any AMAS or reference sampler deployment (5, 6, 9, 13, 14) that had a filter with a low OP ($<100 \text{ pmol min}^{-1} \text{ m}^{-3}$) were excluded from the OP comparisons. The low OP measurements were removed due to the high variability observed in the DTT assay (see Figure S9) at low levels of OP. The percent error between the reference sampler and cumulative AMAS OP concentrations are shown above each set of paired filter data. The error ($\text{MNAE} = 33\%$ and $E_{\text{NMAEF}} = 0.12$) for these data pairs and a Deming regression (Figure S14) demonstrate an overestimation by the AMAS, moderate correlation ($r = 0.43$, $\text{CCC} = 0.39$) and a low bias demonstrated by the Bland-Altman plot (Figure S15, $\text{LoA} = [-119, 81 \text{ pmol min}^{-1} \text{ m}^{-3}]$, $B_{\text{NMBF}} = 0.12$).

We also compared the AMAS BC data to the central site AE33 BC concentration (Figure 5) and mass (Figure S16) estimates by microenvironment for each filter from the 20 valid 48-h deployments with BC measurements above the LOD ($0.49 \mu\text{g}$). To achieve this comparison, the central site BC mass and concentrations were estimated using the hourly AE33 BC concentration data coupled with the AMAS microenvironment designations. One key item worth noting, particularly in the home microenvironment, is the variability in BC exposures between different participants on a given day. The variability of BC concentration (Figures 5 and S16) and mass (Figure S17) is accentuated on days with higher ambient BC. These nuances in the data could indicate exceptional exposure events for some of the participants. An additional item to note is that a consistent bias between the central site measurements and both the traditional personal sampler and AMAS filters (Figure S18) was found on the days with higher ambient BC (11/2–11/4 and 11/08–11/10). This finding agrees with previous studies that suggests indoor microenvironments generally provide some filtration and thus protection from elevated ambient air pollution exposures.⁵³ While there is a chance that this finding could be the result of measurement bias, the personal sampling comparison results (Figure 5) suggest this is not the case.

Strengths and Limitations.

Overall the AMAS demonstrated acceptable accuracy (within $\pm 25\%$ of reference methods⁵¹) for BC detection for samples with sufficient $\text{PM}_{2.5}$ mass when compared to the traditional personal sampler. The AMAS accuracy for OP (33%) fell outside this range, largely due to the limited number of OP samples that passed quality assurance metrics. The participants, in general, were positive about their experience and preferred the AMAS over the traditional personal samplers (based on a usersatisfaction survey; Figure S19). Most importantly the AMAS provided the subtle but important differences in personal exposures that would otherwise be ambiguous if an ambient central-site monitors was the only source of exposure information.

There are several limitations worth noting. First, only 54% of the student participant data collected met our requirements for data analysis. The primary reason for this limitation was tied to the battery life being relatively short and lasting only 14 h before additional charging

was needed. Although compliant participants were often able to maintain the AMAS power for the entire 48-h sampling period, we plan to add an additional battery to the AMAS to extend operating time between charges. An alternative strategy to extend operating lifetime is to reduce sample flow (i.e., pump power requirements) to 1 L min⁻¹ for the home microenvironment; this change, however, may lead to more filter samples below analytic detection limits. Second, the microenvironment classification tended to perform poorly when the transition distance thresholds were on the same order as the GPS signal drift (~200 m). The GPS signal was often slow to connect after long periods (overnight) of having a low quality or null GPS signal. We plan to modify the GPS settings, modify the radii of the microenvironment buffers, and incorporate additional algorithm logic to determine if the sampler was in motion and assist in the detection of microenvironment transitions. Third, the DTT assay would benefit from using a smaller dilution volume than used in this study (500 μ L), which may require alternative methods such as a small-volume electrochemical assay.⁵⁴

The AMAS has been developed and demonstrated the ability to evaluate an individual's BC and OP within individual microenvironments in Fresno, CA. The AMAS is capable of sampling PM onto filter media in distinct microenvironments, and to our knowledge there is no personal sampler with this capability. The ability of this novel personal sampler to collect PM from microenvironments onto filter media permits speciation of PM by microenvironment; thus, providing a new capability for further investigating the impacts of PM composition on health outcomes. An aerosol monitor capable of sampling in distinct microenvironments will allow exposure scientists and epidemiologists to collect more samples and thus provide better insight into the effect of PM composition on human health.

Supplementary Material

Refer to Web version on PubMed Central for supplementary material.

ACKNOWLEDGMENTS

This work was supported by grant ES24719 from the National Institute of Environmental Health Sciences and by grant OH010662 from the National Institute for Occupational Safety and Health. This work was also supported by the Children's Health & Air Pollution Study (CHAPS), an NIH/EPA-funded Children's Environmental Health and Disease Prevention Research Center (EPA: RD83543501, NIH: ES022849). The authors wish to thank all of the student volunteers who helped collect the samples. Additionally, the authors wish to thank The Center for Advanced Research and Technology (CART) and in particular Staci Bynum, Ashley Howell, and Steve Wilson. Finally, the authors would like to acknowledge those who helped with the development of the AMAS, sample collection, and filter processing: Eric Wendt, Jake Lord, James Cao, Jaruwan Mettakoonpitak, Jennifer Mann, Joshua Smith, Laurelle Turner, Michael Nguyen, Nathan Henry, Nicholas Good, Robert Channon, Sarah Sharpe, and Scott Kelleher.

REFERENCES

- (1). Cohen AJ; Brauer M; Burnett R; Anderson HR; Frostad J; Estep K; Balakrishnan K; Brunekreef B; Dandona L; Dandona R Estimates and 25-year trends of the global burden of disease attributable to ambient air pollution: an analysis of data from the Global Burden of Diseases Study 2015. *Lancet* 2017, 389 (10082), 1907–1918. [PubMed: 28408086]
- (2). Pope CA, III; Dockery DW Health effects of fine particulate air pollution: lines that connect. *J. Air Waste Manage. Assoc* 2006, 56 (6), 709–742.
- (3). Brook RD; Rajagopalan S; Pope CA; Brook JR; Bhatnagar A; Diez-Roux AV; Holguin F; Hong Y; Luepker RV; Mittleman MA Particulate matter air pollution and cardiovascular disease: an update

- to the scientific statement from the American Heart Association. *Circulation* 2010, 121 (21), 2331–2378. [PubMed: 20458016]
- (4). Mann JK; Balmes JR; Bruckner TA; Mortimer KM; Margolis HG; Pratt B; Hammond SK; Lurmann FW; Tager IB Short-term effects of air pollution on wheeze in asthmatic children in Fresno, California. *Environ. Health Perspect* 2010, 118 (10), 1497. [PubMed: 20570778]
 - (5). Peel JL; Tolbert PE; Klein M; Metzger KB; Flanders WD; Todd K; Mulholland JA; Ryan PB; Frumkin H Ambient air pollution and respiratory emergency department visits. *Epidemiology* 2005, 16 (2), 164–174. [PubMed: 15703530]
 - (6). Wilson JG; Kingham S; Pearce J; Sturman AP A review of intraurban variations in particulate air pollution: Implications for epidemiological research. *Atmos. Environ* 2005, 39 (34), 6444–6462.
 - (7). Branco P; Alvim-Ferraz M; Martins F; Sousa S The microenvironmental modelling approach to assess children's exposure to air pollution—A review. *Environ. Res* 2014, 135, 317–332. [PubMed: 25462682]
 - (8). Dons E; Panis LI; Van Poppel M; Theunis J; Willems H; Torfs R; Wets G Impact of time–activity patterns on personal exposure to black carbon. *Atmos. Environ* 2011, 45 (21), 3594–3602.
 - (9). Lim S; Kim J; Kim T; Lee K; Yang W; Jun S; Yu S Personal exposures to PM 2.5 and their relationships with microenvironmental concentrations. *Atmos. Environ* 2012, 47, 407–412.
 - (10). Van Ryswyk K; Wheeler AJ; Wallace L; Kearney J; You H; Kulka R; Xu X Impact of microenvironments and personal activities on personal PM 2.5 exposures among asthmatic children. *J. Exposure Sci. Environ. Epidemiol* 2014, 24 (3), 260.
 - (11). Health Effects Institute. *Traffic-Related Air Pollution: A Critical Review of the Literature on Emissions, Exposure, And Health Effects, Special Report 17*; Health Effects Institute: 2010.
 - (12). Hoek G; Beelen R; De Hoogh K; Vienneau D; Gulliver J; Fischer P; Briggs D A review of land-use regression models to assess spatial variation of outdoor air pollution. *Atmos. Environ* 2008, 42 (33), 7561–7578.
 - (13). Jedynska A; Hoek G; Wang M; Yang A; Eeftens M; Cyrys J; Keuken M; Ampe C; Beelen R; Cesaroni G Spatial variations and development of land use regression models of oxidative potential in ten European study areas. *Atmos. Environ* 2017, 150, 24–32.
 - (14). Dons E; Van Poppel M; Kochan B; Wets G; Panis LI Modeling temporal and spatial variability of traffic-related air pollution: Hourly land use regression models for black carbon. *Atmos. Environ* 2013, 74, 237–246.
 - (15). Michanowicz DR; Shmool JL; Tunno BJ; Tripathy S; Gillooly S; Kinnee E; Clougherty JE A hybrid land use regression/AERMOD model for predicting intra-urban variation in PM2. 5. *Atmos. Environ* 2016, 131, 307–315.
 - (16). Schulte JK; Fox JR; Oron AP; Larson TV; Simpson CD; Paulsen M; Beaudet N; Kaufman JD; Magzamen S Neighborhood-scale spatial models of diesel exhaust concentration profile using 1-nitropyrene and other nitroarenes. *Environ. Sci. Technol* 2015, 49 (22), 13422–13430. [PubMed: 26501773]
 - (17). Good N; Mölter A; Ackerson C; Bachand A; Carpenter T; Clark ML; Fedak KM; Kayne A; Koehler K; Moore B The Fort Collins Commuter Study: Impact of route type and transport mode on personal exposure to multiple air pollutants. *J. Exposure Sci. Environ. Epidemiol* 2016, 26 (4), 397–404.
 - (18). Ham W; Vijayan A; Schulte N; Herner JD Commuter exposure to PM2. 5, BC, and UFP in six common transport microenvironments in Sacramento, California. *Atmos. Environ* 2017, 167, 335–345.
 - (19). Steinle S; Reis S; Sabel CE Quantifying human exposure to air pollution—moving from static monitoring to spatio-temporally resolved personal exposure assessment. *Sci. Total Environ* 2013, 443, 184–193. [PubMed: 23183229]
 - (20). Larkin A; Hystad P Towards personal exposures: how technology is changing air pollution and health research. *Current Environmental Health Reports* 2017, 4 (4), 463–471. [PubMed: 28983874]
 - (21). Koehler KA; Peters TM New methods for personal exposure monitoring for airborne particles. *Current environmental health reports* 2015, 2 (4), 399–411. [PubMed: 26385477]

- (22). Bell ML; Ebisu K; Leaderer BP; Gent JF; Lee HJ; Koutrakis P; Wang Y; Dominici F; Peng RD Associations of PM_{2.5} constituents and sources with hospital admissions: analysis of four counties in Connecticut and Massachusetts (USA) for persons ≥ 65 years of age. *Environ. Health Perspect* 2014, 122 (2), 138. [PubMed: 24213019]
- (23). Secrest MH; Schauer JJ; Carter EM; Lai AM; Wang Y; Shan M; Yang X; Zhang Y; Baumgartner J The oxidative potential of PM_{2.5} exposures from indoor and outdoor sources in rural China. *Sci. Total Environ* 2016, 571, 1477–1489. [PubMed: 27443462]
- (24). Charrier JG; Anastasio C Rates of hydroxyl radical production from transition metals and quinones in a surrogate lung fluid. *Environ. Sci. Technol* 2015, 49 (15), 9317–9325. [PubMed: 26153923]
- (25). Arku RE; Birch A; Shupler M; Yusuf S; Hystad P; Brauer M Characterizing exposure to household air pollution within the Prospective Urban Rural Epidemiology (PURE) study. *Environ. Int.* 2018, 114, 307–317. [PubMed: 29567495]
- (26). Carter E; Norris C; Dionisio KL; Balakrishnan K; Checkley W; Clark ML; Ghosh S; Jack DW; Kinney PL; Marshall JD Assessing exposure to household air pollution: a systematic review and pooled analysis of carbon monoxide as a surrogate measure of particulate matter. *Environ. Health Perspect* 2017, 125 (7), 076002 [PubMed: 28886596]
- (27). Adams C; Riggs P; Volckens J Development of a method for personal, spatiotemporal exposure assessment. *J. Environ. Monit* 2009, 11 (7), 1331–1339. [PubMed: 20449221]
- (28). Rabinovitch N; Adams CD; Strand M; Koehler K; Volckens J Within-microenvironment exposure to particulate matter and health effects in children with asthma: a pilot study utilizing realtime personal monitoring with GPS interface. *Environ. Health* 2016, 15 (1), 96. [PubMed: 27724963]
- (29). Steinle S; Reis S; Sabel CE; Semple S; Twigg MM; Braban CF; Leeson SR; Heal MR; Harrison D; Lin C Personal exposure monitoring of PM_{2.5} in indoor and outdoor microenvironments. *Sci. Total Environ* 2015, 508, 383–394. [PubMed: 25497678]
- (30). Carvlin GN; Lugo H; Olmedo L; Bejarano E; Wilkie A; Meltzer D; Wong M; King G; Northcross A; Jerrett M Development and field validation of a community-engaged particulate matter air quality monitoring network in Imperial, California, USA. *J. Air Waste Manage. Assoc* 2017, 67 (12), 1342–1352.
- (31). Northcross AL; Edwards RJ; Johnson MA; Wang Z-M; Zhu K; Allen T; Smith KR A low-cost particle counter as a realtime fine-particle mass monitor. *Environmental Science: Processes & Impacts* 2013, 15 (2), 433–439. [PubMed: 25208708]
- (32). Ryan PH; Son SY; Wolfe C; Lockey J; Brokamp C; LeMasters G A field application of a personal sensor for ultrafine particle exposure in children. *Sci. Total Environ* 2015, 508, 366–373. [PubMed: 25497676]
- (33). Rivas I; Donaire-Gonzalez D; Bouso L; Esnaola M; Pandolfi M; de Castro M; Viana M; Álvarez-Pedrerol M; Nieuwenhuijsen M; Alastuey A Spatiotemporally resolved black carbon concentration, schoolchildren's exposure and dose in Barcelona. *Indoor air* 2016, 26 (3), 391–402. [PubMed: 25924870]
- (34). Chartier R; Phillips M; Mosquin P; Elledge M; Bronstein K; Nandasena S; Thornburg V; Thornburg J; Rodes C A comparative study of human exposures to household air pollution from commonly used cookstoves in Sri Lanka. *Indoor air* 2017, 27 (1), 147–159. [PubMed: 26797964]
- (35). Chow JC; Watson JG; Green MC; Frank NH Filter light attenuation as a surrogate for elemental carbon. *J. Air Waste Manage. Assoc* 2010, 60 (11), 1365–1375.
- (36). Künzli N; Mudway IS; Götschi T; Shi T; Kelly FJ; Cook S; Burney P; Forsberg B; Gauderman JW; Hazenkamp ME Comparison of oxidative properties, light absorbance, and total and elemental mass concentration of ambient PM_{2.5} collected at 20 European sites. *Environ. Health Perspect* 2005, 114 (5), 684.
- (37). Presler-Jur P; Doraiswamy P; Hammond O; Rice J An evaluation of mass absorption cross-section for optical carbon analysis on Teflon filter media. *J. Air Waste Manage. Assoc* 2017, 67 (11), 1213–1228.
- (38). Sameenoi Y; Panymeesamer P; Supalakorn N; Koehler K; Chailapakul O; Henry CS; Volckens J Microfluidic paper-based analytical device for aerosol oxidative activity. *Environ. Sci. Technol.* 2013, 47 (2), 932–940. [PubMed: 23227907]

- (39). Charrier JG; McFall AS; Vu KK; Baroi J; Olea C; Hasson A; Anastasio C A bias in the “mass-normalized” DTT response—An effect of non-linear concentration-response curves for copper and manganese. *Atmos. Environ* 2016, 144, 325–334.
- (40). Fang T; Verma V; Guo H; King L; Edgerton E; Weber R A semi-automated system for quantifying the oxidative potential of ambient particles in aqueous extracts using the dithiothreitol (DTT) assay: results from the Southeastern Center for Air Pollution and Epidemiology (SCAPE). *Atmos. Meas. Tech* 2015, 8 (1), 471–482.
- (41). Volckens J; Quinn C; Leith D; Mehaffy J; Henry CS; Miller-Lionberg D Development and evaluation of an ultrasonic personal aerosol sampler. *Indoor air* 2017, 27 (2), 409–416. [PubMed: 27354176]
- (42). Colorado State University CSU UPAS Android App. <https://play.google.com/store/apps/details?id=app.volckensgroup.UPASv2&hl=en> (Nov 2017).
- (43). Colorado State University CSU UPAS iOS App. <https://itunes.apple.com/us/app/csu-upas/id1126067765?mt=8> (Nov 2017).
- (44). Kahle D; Wickham H ggmap: Spatial Visualization with ggplot2. *R Journal* 2013, 5, (1).
- (45). Drinovec L; Mo nik G; Zotter P; Prévôt A; Ruckstuhl C; Coz E; Rupakheti M; Sciare J; Müller T; Wiedensohler A. The “ dual-spot ” Aethalometer: an improved measurement of aerosol black carbon with real-time loading compensation. *Atmos. Meas. Tech* 2015, 8 (5), 1965–1979.
- (46). Exposure Factors Handbook 2011 ed. (Final Report), EPA/600/ R-09/052F; United States Environmental Protection Agency: Washington D.C., 2011.
- (47). Abrams JY; Weber RJ; Klein M; Sarnat SE; Chang HH; Strickland MJ; Verma V; Fang T; Bates JT; Mulholland JA Associations between Ambient Fine Particulate Oxidative Potential and Cardiorespiratory Emergency Department Visits. *Environ. Health Perspect.* 2017, 125 (12), 129001 [PubMed: 29212063]
- (48). Weichenthal SA; Lavigne E; Evans GJ; Godri Pollitt KJ; Burnett RT Fine particulate matter and emergency room visits for respiratory illness. Effect modification by oxidative potential. *Am. J. Respir. Crit. Care Med* 2016, 194 (5), 577–586. [PubMed: 26963193]
- (49). Cho AK; Sioutas C; Miguel AH; Kumagai Y; Schmitz DA; Singh M; Eiguren-Fernandez A; Froines JR Redox activity of airborne particulate matter at different sites in the Los Angeles Basin. *Environ. Res* 2005, 99 (1), 40–47. [PubMed: 16053926]
- (50). Yu S; Eder B; Dennis R; Chu SH; Schwartz SE New unbiased symmetric metrics for evaluation of air quality models. *Atmospheric Science Letters* 2006, 7 (1), 26–34.
- (51). Kennedy ER; Fischbach TJ; Song R; Eller PM; Shulman SA Guidelines for Air Sampling and Analytical Method Development and Evaluation; National Inst. for Occupational Safety and Health: Cincinnati, OH, 1994.
- (52). Breen MS; Long TC; Schultz BD; Crooks J; Breen M; Langstaff JE; Isaacs KK; Tan Y-M; Williams RW; Cao Y GPS-based microenvironment tracker (MicroTrac) model to estimate time –location of individuals for air pollution exposure assessments: Model evaluation in central North Carolina. *J. Exposure Sci. Environ. Epidemiol.* 2014, 24 (4), 412.
- (53). Guarnieri M; Balmes JR Outdoor air pollution and asthma. *Lancet* 2014, 383 (9928), 1581–1592. [PubMed: 24792855]
- (54). Koehler KA; Shapiro J; Sameenoi Y; Henry C; Volckens J Laboratory Evaluation of a Microfluidic Electrochemical Sensor for Aerosol Oxidative Load. *Aerosol Sci. Technol* 2014, 48 (5), 489–497. [PubMed: 24711675]

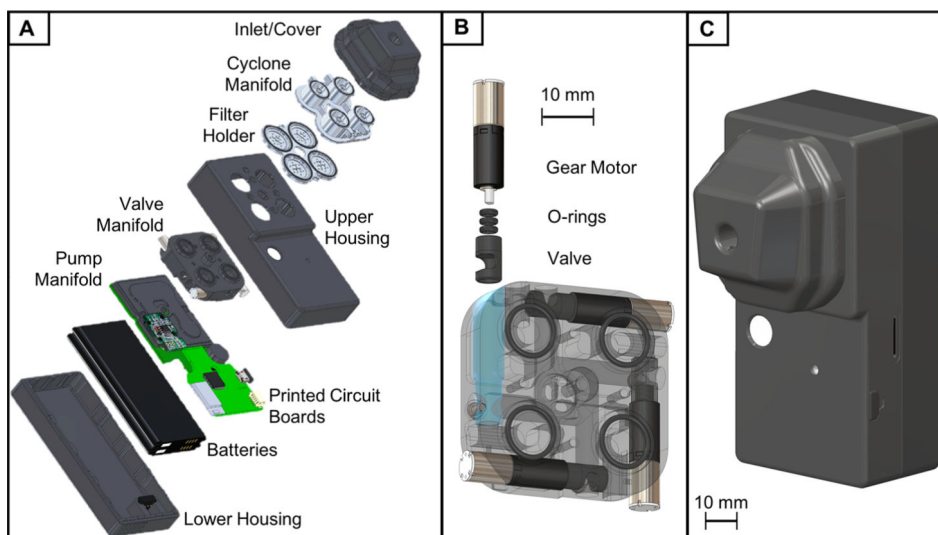


Figure 1. AMAS design and hardware. (A) Exploded view of all hardware components. (B) Partial exploded view of the valve manifold. (C) Fully assembled AMAS prototype.

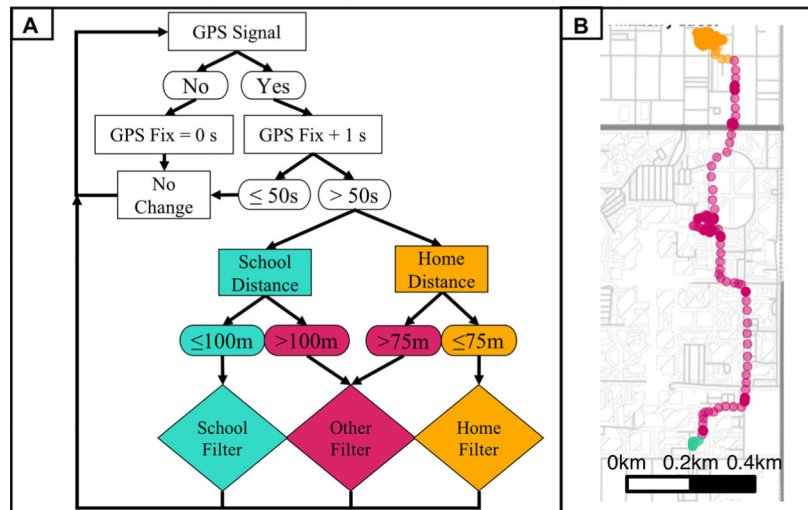


Figure 2.

(A) AMAS algorithm used to determine the microenvironment location (school, home, or other) and to initiate sample collection into the corresponding filter channel. (B) An example trace is shown to demonstrate home, school, and other microenvironments (orange, green, and red respectively). The map was generated with the `ggmap`⁴⁴ library using R 3.4.1 (R Core Team, Vienna, Austria).

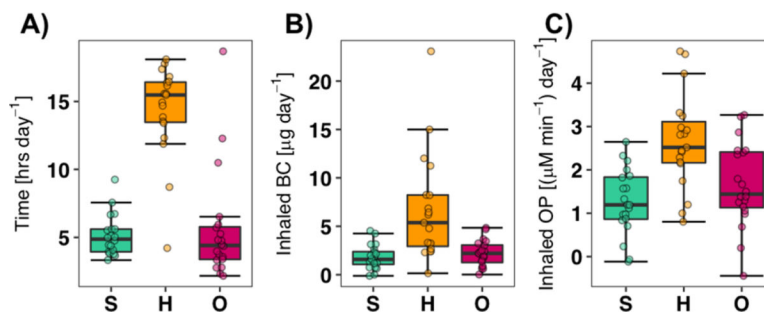


Figure 3. Microenvironment exposure results (school = S; home = H; other = O). Data are shown only for AMAS that were collected by participants, sampled the entire 48-h period, had valid GPS coordinates, and collected PM_{2.5} for more than an hour (0.1 m³) in each microenvironment ($n = 20, 19, 20$ for S, H, and O). A) Daily time spent in microenvironments as detected by the algorithm. B) Daily inhaled black carbon mass. C) Daily oxidative potential reactivity of the inhaled PM_{2.5}.

Author Manuscript

Author Manuscript

Author Manuscript

Author Manuscript

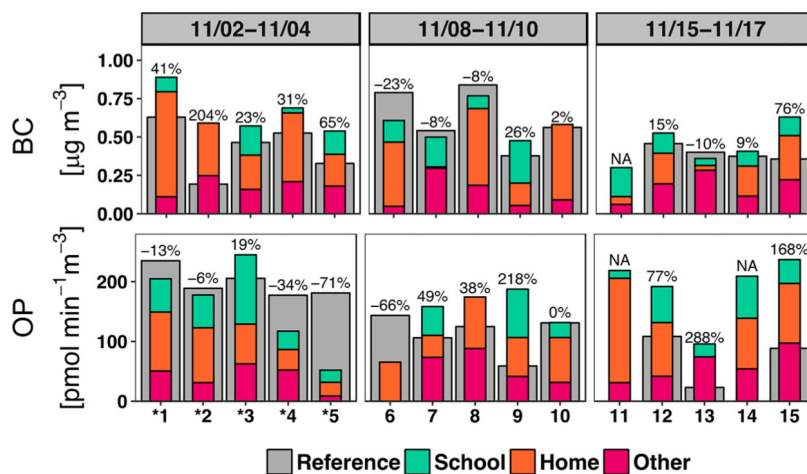


Figure 4. Comparison of the traditional personal sampler (Reference) and AMAS 48-h concentrations for BC and OP. The percent error between the AMAS cumulative concentration and the reference sampler concentrations for the 48-h periods is listed above each bar. Filter pairs 1–5 had MTL Teflon filters for the traditional personal sampler. All other reference filters and all AMAS filters were Pallflex Fiberfilm™.

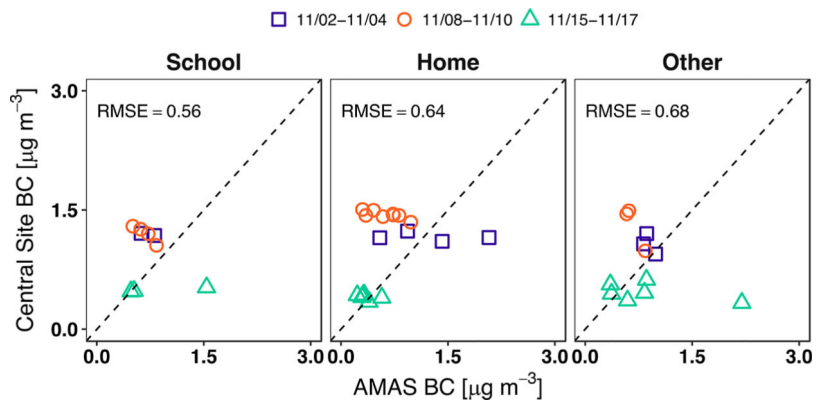


Figure 5. Central site BC concentrations compared to AMAS filter BC concentrations by microenvironment. The data shown in the plots include only filter samples from deployments which collected $\text{PM}_{2.5}$ and AMAS data for the entire 48-h period, had valid GPS coordinates, collected $\text{PM}_{2.5}$ for more than an hour (0.1 m^3) in each microenvironment, and the BC measurement was above the LOD ($0.49 \mu\text{g}$) of the Magee Scientific Sootscan measurement (school, $n = 9$; home, $n = 18$; other, $n = 12$). The RMSE is shown in each microenvironment panel and the dashed line is the 1:1 reference line.